*Thin Solid Films*, 99 (1983) 379–384


# THICKNESS VARIATIONS OF RESISTANCE AND ACTIVATION ENERGY IN VERY THIN DISCONTINUOUS METAL FILMS

G. O. SVARSTAD*, L. D. FEISEL AND J. E. MORRIS

*Department of Electrical Engineering, South Dakota School of Mines and Technology, Rapid City, SD 57701 (U.S.A.)*

(Received February 16, 1982; accepted July 13, 1982)

The electrical resistance and activation energy of conduction in discontinuous gold films have been determined as functions of thickness in the very early stages of deposition. Both display abrupt changes of slope which could be taken as an indication of the saturation thickness $t_s$, except that the changes do not occur at the same thickness. A tentative explanation is proposed based on field-induced coalescence.

## 1. INTRODUCTION

The growth of a vacuum-deposited thin metal film can be considered to consist of four separate phases. In the first phase, deposited atoms are adsorbed by the substrate to form critical nuclei. Prior to adsorption, the atom loses energy by movement on the substrate surface but is unlikely to be captured by any of the few existing nuclei. Establishment of an array of stable supercritical nuclei continues until the separation $s$ between them approaches twice the "capture distance" of a stable nucleus. At this point, any new atom arriving on the substrate surface will encounter an existing supercritical nucleus (island) and be absorbed by it before adsorption by the substrate. The island density is now said to be saturated at the saturation thickness $t_s$. The second phase of island growth then begins with addition of metal atoms either directly from the vapor or by capture from the surrounding substrate surface. There may also be some coalescence of islands in this part of the sequence before the critical thickness $t_c$ is reached, when the film resistance falls sharply. As the islands grow, the separation decreases and strings of islands develop into continuous filaments. At $t_c$, a continuous metallic path through the film exists for the first time. Beyond $t_c$, the voids in the film fill in in the third phase followed by the conventional increase in thickness (fourth stage) of a continuous layer. The variation in resistance expected during the first three phases is shown in Fig. 1. Resistance changes around $t_c$ have been extensively discussed by other researchers[1–6]. This paper is concerned with film resistance at lower thicknesses.

For thickness less than $t_c$, the film is discontinuous, consisting of discrete metal

* Present address: Black Hills Power and Light Co., Deadwood Avenue, Rapid City, SD 57701, U.S.A.

0040-6090/83/0000-0000/$03.00 

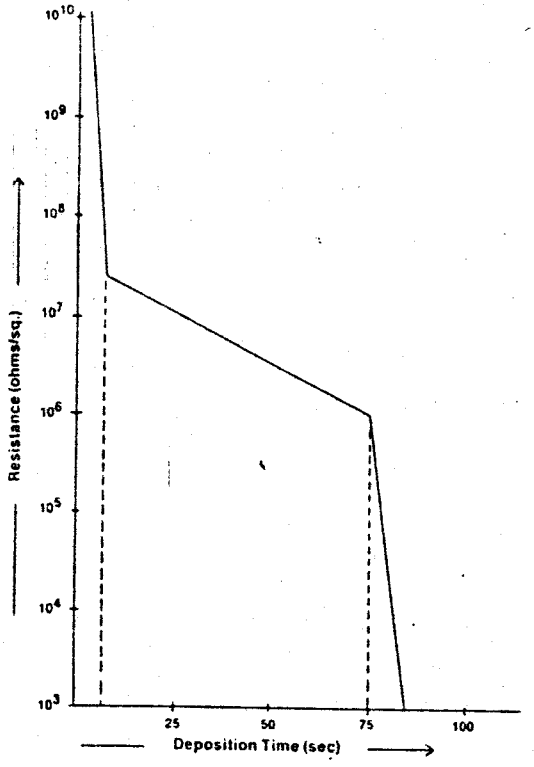


Fig. 1. Typical deposition curve (schematic).

islands. Electrical conduction between the islands takes place by electron tunneling through the substrate (or surface). There are still many details of the process which are unclear[7] but the film resistance $R$ at an absolute temperature $T$ may still be adequately described by[8]

$$\ln R = \lambda + \frac{4\pi}{h}(2m^*\bar{\phi})^{1/2}s + \frac{\delta E}{kT} \tag{1}$$

where $\lambda$ is only weakly dependent on $s$, $m^*$ is the effective mass of the tunneling electron, $\bar{\phi}$ is the effective potential barrier between islands, $h$ is Planck's constant, the electrostatic activation energy $\delta E = (e^2/4\pi\varepsilon)\{r^{-1} - (r+s)^{-1}\}$, $e$ is the electronic charge, $\varepsilon \approx \varepsilon_0$ is the effective dielectric constant, $r$ is the radius of the (assumed) hemispherical islands and $k$ is Boltzmann's constant.

## 2. EXPERIMENTAL TECHNIQUE AND RESULTS

Experimental variations in film resistance and activation energy as the thickness increases through $t_c$ are presented in Figs. 2 and 3, where the gold films were resistively evaporated at rates of around 0.1 nm $s^{-1}$ with a background vapor pressure of $2 \times 10^{-7}$ Torr. The vacuum system was sputter ion pumped with sorption roughing to an ultimate pressure of $10^{-8}$ Torr. Apart from the Viton A bell-jar seal, all gaskets were metal and all fittings stainless steel or copper. Glazed

Fig. 3. Activation energy variation with average thickness about $t_c$ (the films are the same as for Fig. 2; pressure, $2 \times 10^{-5}$ Torr).




Fig. 2. Deposition curves: film resistance variations with average thickness about $t_c$. Points where the activation energies were measured (Fig. 3) are marked. The system pressure during deposition was $2 \times 10^{-7}$ Torr.

AlSiMag 743 substrates were used with surface resistivities in excess of $10^{10}$ Ω/□ and less than 1 μin surface roughness. Thin film thermocouples of 99.95%Ni/99.9%Cu were deposited alongside the discontinuous gold film to monitor the surface temperature. The substrates were heated from behind with quartz IR heaters. The average thickness of the discontinuous gold film was measured with a quartz crystal in the plane of the film (but offset 3.2 cm to the side) and a Sloan DTM2A monitor. Crystal frequency changes were calibrated against film thicknesses measured by multiple-beam interferometry to 5% accuracy. The 1 nm accuracy of the Sloan DTM2A was improved to 0.1 nm by the addition of a HP 5245L digital counter. The film resistance was measured *in vacuo* with a four-point probe. During deposition, at rates of below 0.1 nm $s^{-1}$, a Keithley 600A electrometer was used with remote output recording. At higher rates, a Fluke 8100A digital multimeter was set up alongside the digital thickness meter for video recording of both displays for later analysis by slow playback. The final accuracy in the activation energies is dominated by the temperature measurement and has been estimated at 5%–10%.

The conventional method[8] of obtaining such data (Figs. 2 and 3) is to stop deposition, to cycle the film temperature to determine $\delta E$ and then to continue deposition. However, it is known that the film geometry continues to change after deposition ceases and therefore the film properties must change during this interruption of the normal deposition. The technique adopted here was to use totally separate depositions, *i.e.* separate films, for each determination of $\delta E$. Three films could be deposited in a single pumpdown. Each film deposition was terminated at a predetermined time and a 50 nm overlayer of silicon oxide immediately deposited to "lock" the structure and to prevent structural change or surface contamination. (The silicon oxide is presumed to condense as $SiO_x$, $1 < x < 2$.)

The silicon oxide does affect both the film resistance (which typically decreases to 2/3 of its original value) and the activation energy (which decreases by less than 8%), but these changes have been found to be reasonably consistent[9]. The most important requirement for utilizing different films in this way is the ability to reproduce film structures and properties reliably by control of the deposition conditions. Apart from the usual control parameters (substrate temperature, deposition rate), particular attention was paid to consistency of the background vacuum system pressure during deposition. This has been found to have a strong influence on the form of the deposition curve[9], probably due to substrate surface contamination. Routine substrate cleaning was also performed (scrub with Alconox detergent solution, water rinse for 5 min, vapor degrease in isopropyl alcohol, dry in nitrogen), but the actual deposition surface was the top of a 500 nm layer of silicon oxide deposited on the substrate immediately prior to metal film evaporation. This technique provides very consistent data.

## 3. INTERPRETATION OF RESULTS

The discontinuities in both Fig. 2 and Fig. 3 seem to indicate that the saturation thickness has been reached, fast changes in $R$ and $\delta E$ being consistent with rapid variation in the island separation $s$ as new nuclei develop within existing gaps. By contrast, once the nucleus density has stabilized, the gap width changes more slowly as existing islands grow. Further analysis of the results in terms of this model,

however, produces some inconsistencies. The plots of Figs. 2 and 3 which appear so simple to interpret in terms of $t_s$ are shown by Fig. 4 to involve more complex processes than described above. Close inspection of Figs. 2 and 3 shows that there are actually two separate discontinuities.

Equation (1) may be differentiated to give

$$\frac{d(\ln R)}{dt} - \frac{d}{dt}\left(\frac{\delta E}{kT}\right) = \frac{4\pi}{h}(2m^*\bar{\phi})^{1/2}\frac{ds}{dt} \qquad (2)$$

The differences between the slopes of corresponding plots in Figs. 2 and 3 are plotted in Fig. 4, where similar results are obtained for both films. The data do not appear to be the spurious results of slope errors. (Assuming the rest mass of an electron and 0.5 eV for $\bar{\phi}$, the vertical scale corresponds roughly to $ds/dt$ in nanometers per second.) The essential points are that $ds/dt$ is positive for $t < 5$ s where a large negative transient occurs before settling to lower values associated with island coalescence up to the critical thickness $t_c$.

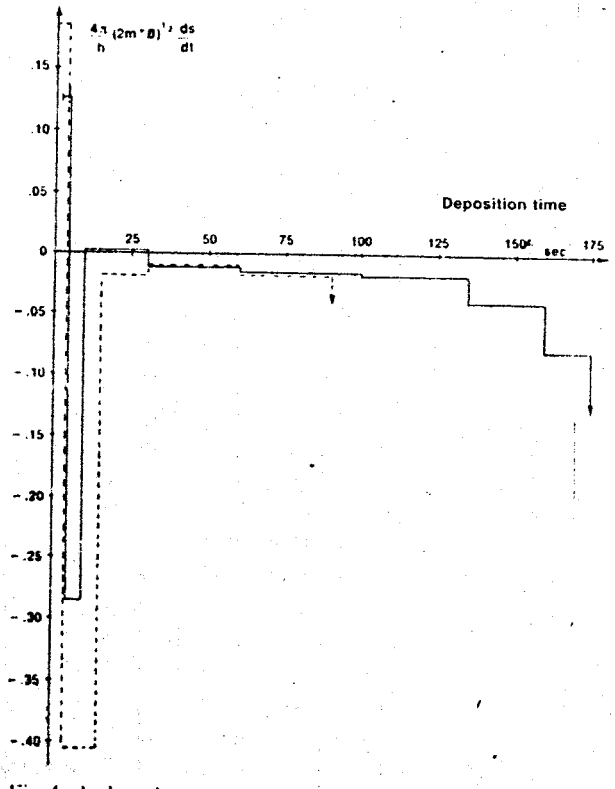


Fig. 4. $ds/dt$ as determined by differences in slope from Figs. 2 and 3: ——, 300 °C; – – –, 150 °C.

For single-atom critical nuclei and a capture distance of 0.5 nm, $t_s$ should be reached in just under 2 s. Allowing for re-evaporation, either discontinuity could correspond to $t_s$ at a value comparable with other published saturation thicknesses[10]. However, the existence of the positive value of $ds/dt$ is evidence that $t_s$ has

already been exceeded at this thickness range (deposition time, 2–5 s), implying negligible re-evaporation. This stage of deposition is characterized by rapidly falling resistances (Fig. 2) dominated by fast changes in $\delta E$ (Fig. 3), which must be partially offset by the positive $ds/dt$. (Provided that $s \geq r$ at this point, the expression

$$(r+s)\frac{1}{\delta E}\frac{d(\delta E)}{dt} = -\frac{dr}{dt}\left(2+\frac{s}{r}\right)+\frac{ds}{dt}\frac{r}{s} \tag{3}$$

shows that $\delta E$ may still decrease with positive $ds/dt$.)

## 4. FIELD-INDUCED COALESCENCE

The problem is to explain the sudden large negative value of $ds/dt$ as shown in Fig. 4. The film resistance was monitored electrically during deposition with a field of 4 V cm$^{-1}$ and a possible explanation of this phenomenon is electric-field-induced coalescence of islands in the conduction path[11–13]. These results would then assume significance in that they would indicate the stage of growth at which field-induced coalescence occurs.

Various models have been used to explain field-induced coalescence: island "stretching", stray charge effects[12,14,15] and electromagnetic polarization[16]. All of these predict repulsive forces between islands at smaller island sizes and wide gaps. This effect can be visualized as producing movement among an irregular island array to increase the separation $s$ as observed for $t < 5$ s.

Beyond the point of rapid coalescence, both $\delta E$ and the resistance variations slow, demonstrating the more expected orderly decrease in $s$ toward the critical thickness.

In summary, (i) both film resistance and activation energy curves undergo changes of shape at thicknesses a little greater than $t_c$, (ii) analysis of the data shows that gap widths are increasing immediately prior to this point where they suddenly decrease dramatically and (iii) a tentative explanation based on field-induced coalescence has been proposed.

## REFERENCES


1 T. J. Coutts, *Thin Solid Films*, *4* (1969) 429–443.
2 T. J. Coutts and B. Hopewell, *Thin Solid Films*, *9* (1971) 37–55.
3 T. J. Coutts, *Electrical Conduction in Thin Metal Films*, Elsevier, Amsterdam, 1974.
4 T. Andersson, *Thin Solid Films*, *29* (1975) L21–L23.
5 T. Andersson, *J. Appl. Phys.*, *47* (1976) 1752.
6 T. Andersson, *J. Phys. D*, *9* (1976) 973–985.
7 J. E. Morris and T. J. Coutts, *Thin Solid Films*, *47* (1977) 1–65.
8 C. A. Neugebauer and M. B. Webb, *J. Appl. Phys.*, *33* (1962) 74–82.
9 G. O. Svarstad, *Ph.D. Thesis*, South Dakota School of Mines and Technology, 1974.
10 A. J. Donohoe and J. L. Robins, *J. Cryst. Growth*, *17* (1972) 70.
11 E. Ahilea and A. A. Hirsch, *J. Appl. Phys.*, *42* (1971) 5601–5608.
12 K. L. Chopra, *J. Appl. Phys.*, *37* (1966) 2249–2254.
13 J. E. Morris, *Metallography*, *5* (1972) 41–58.
14 R. B. Marcus and W. B. Joyce, *Thin Solid Films*, *10* (1972) 1–10.
15 D. B. Dove, *J. Appl. Phys.*, *35* (1964) 2785–2786.
16 G. Desrousseaux, *Thin Solid Films*, *32* (1976) 255–258.